

Electronic supplementary information (ESI)

Coating gold nanorods with silica prevents the generation of reactive oxygen species under laser light irradiation for safe biomedical applications

Sarra Mitiche^a, Syrine Gueffrache^a, Sylvie Marguet^b, Jean-Frédéric Audibert^c, Robert Bernard Pansu^a, Bruno Palpant^{a*}

^a Université Paris-Saclay, CNRS, ENS Paris-Saclay, CentraleSupélec, LuMIn, 91190 Gif-sur-Yvette, France

^b Université Paris-Saclay, CEA, CNRS, NIMBE, 91190 Gif-sur-Yvette, France

^c Université Paris-Saclay, CNRS, ENS Paris-Saclay, PPSM, 91190 Gif-sur-Yvette, France

* Corresponding author.

E-mail address: bruno.palpant@universite-paris-saclay.fr

I. Additional images of the silica-coated gold nanorods (AuNRs@SiO₂)

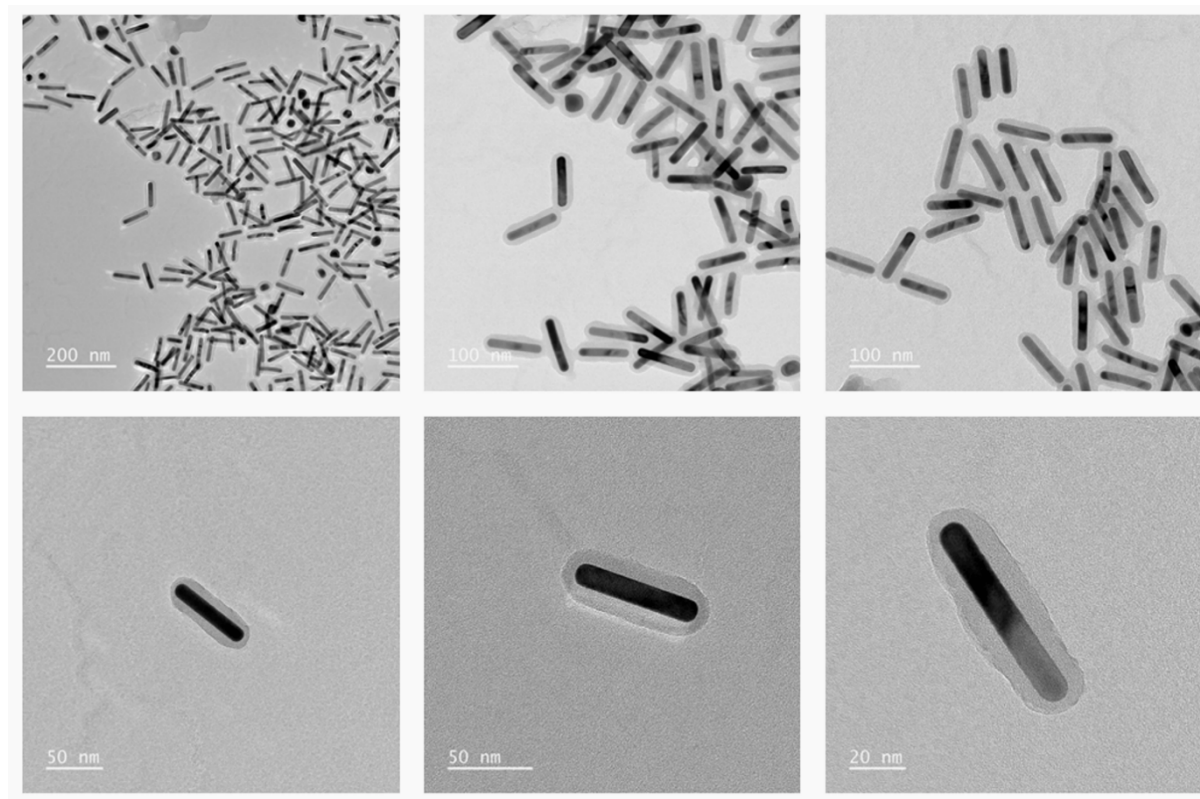


Fig. S1. TEM images of AuNRs@SiO₂. Average dimensions: 12.2 ± 1.3 nm thick and 73.0 ± 8.3 nm long. The average thickness of the silica coating is 8.7 ± 1.3 nm.

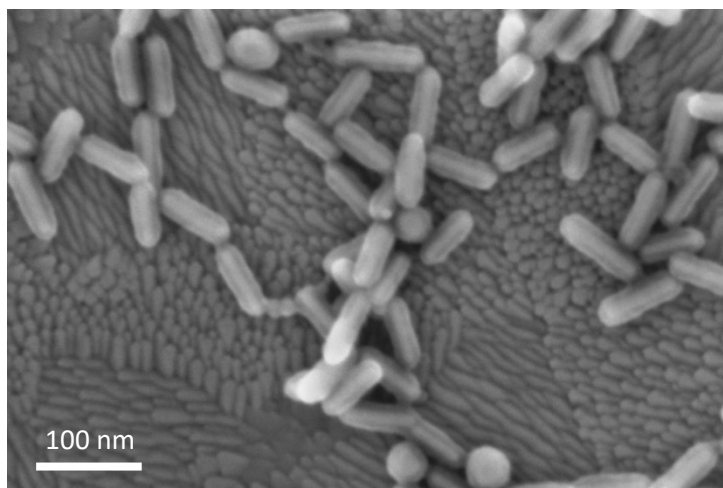


Fig. S2. SEM image of AuNRs@SiO₂. Average dimensions: 12.2 ± 1.3 nm thick and 73.0 ± 8.3 nm long. The average thickness of the silica coating is 8.7 ± 1.3 nm.

II. Method of inserting the solution into the capillary

The procedure for preparing the sample capillary is summarized in Fig. S3:

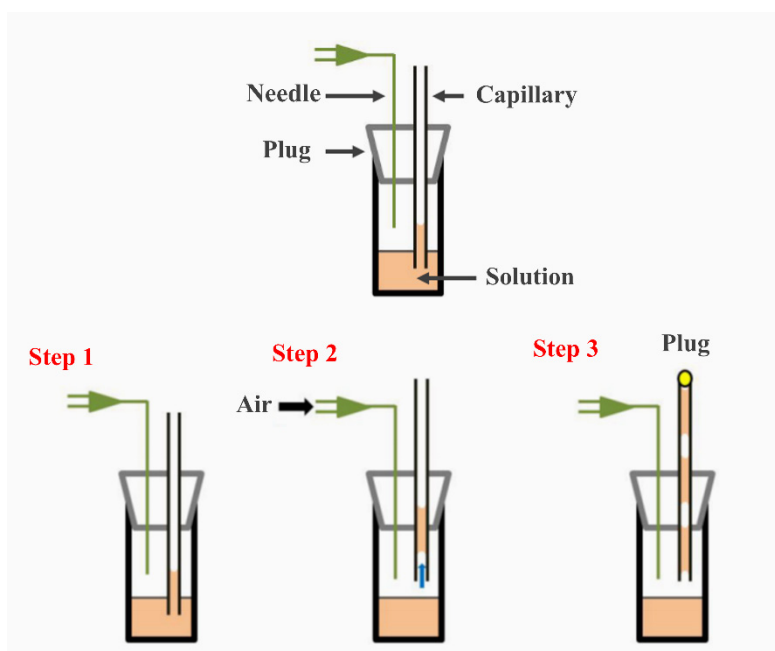


Fig. S3. Procedure for preparing the sample capillary.¹

1. 1 ml of solution is introduced into a glass flask. The flask is then closed with a plug pierced with two holes.
2. In one of the holes, we introduce the capillary and in the other, a syringe needle connected to an air tank.
3. The end of the capillary is immersed into the solution and a drop of solution rises in the capillary.
4. We take the capillary out of the solution and we introduce air through the needle. A small volume of air rises in the capillary and pushes the drop.
5. We repeat the two previous steps two more times to have three drops in the capillary. The experiments are conducted on the middle drop. The two lateral drops are added in order to limit the gas exchanges between the external environment and the drop under investigation.
6. We take the capillary out of the flask and immediately seal it with two putty plugs.

III. Additional experimental data: AuNRs@SiO₂ with a 5.0-nm silica shell

Additional experimental data are provided in this section to show the reproducibility of the results depicted in Fig. 3 and Fig. 4 of the article. The additional data are obtained for nanoparticles different from those employed in the article. The nanoparticles used in this case are PEGylated AuNRs and AuNRs@SiO₂ 10.2 ± 1.0 nm thick and 61.3 ± 7.2 nm long, dispersed in water. The thickness of the silica coating is 5 nm. The extinction spectra are given in Fig. S4. The longitudinal LSPR of the PEGylated AuNRs and the AuNRs@SiO₂ are respectively 995 nm and 1050 nm. The registered SOSG and DHR emission intensities before, during, and after the excitation of the NP longitudinal LSPR are depicted in Fig. S5 and S6, respectively. The results obtained are in agreement with those in the article.

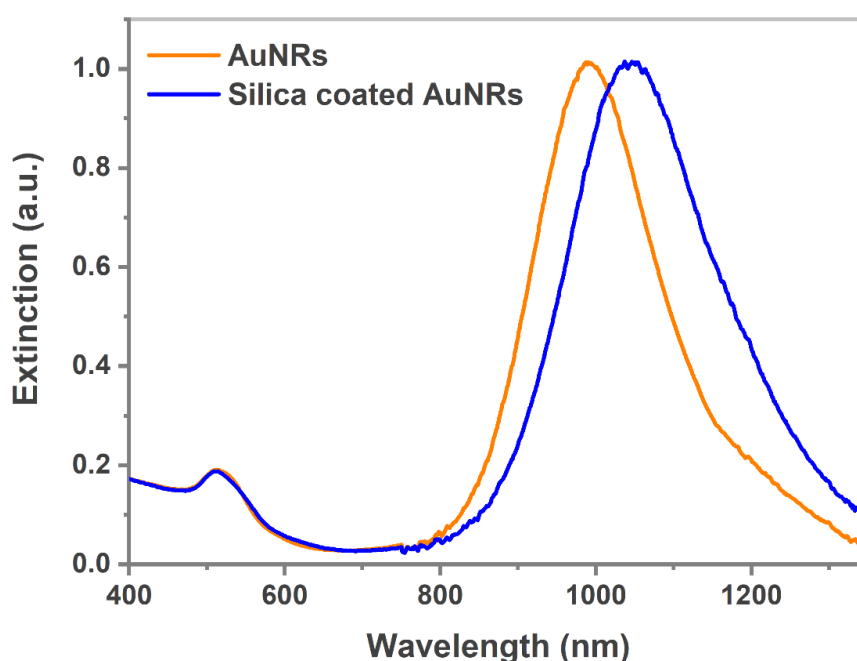


Fig. S4. Extinction spectra of the AuNRs stabilized by HS-PEG ligands in water (orange curve) and the AuNRs@SiO₂ in water (blue curve) with longitudinal LSPR peaks observed at 995 nm and 1050 nm, respectively.

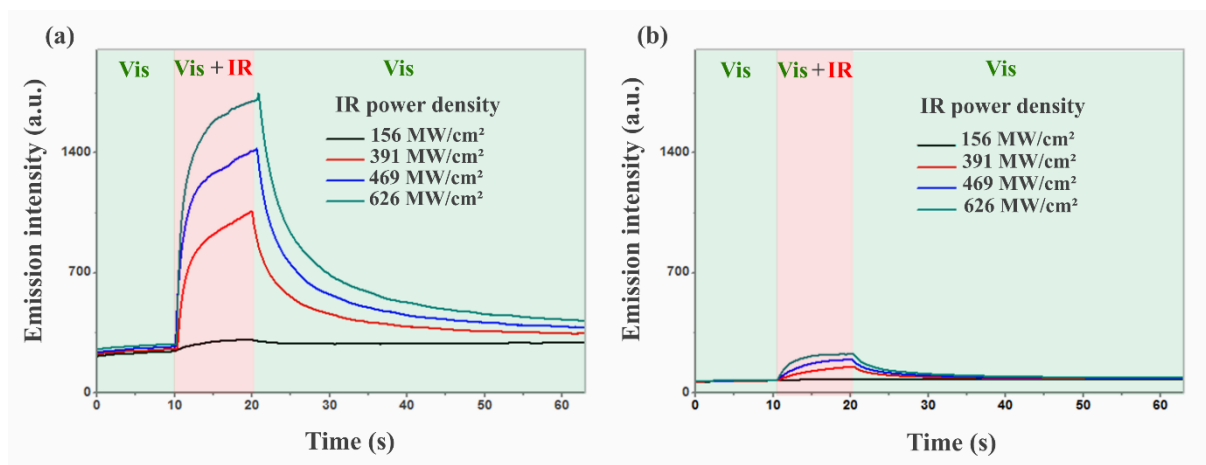


Fig. S5. SOSG emission intensity in the presence of (a) PEGylated AuNRs and (b) AuNRs@SiO₂ acting as ROS photosensitizers, in water. The SOSG reagent detects ¹O₂. The SOSG fluorescence is recorded before, during, and after the excitation of the nanoparticle (NP) longitudinal LSPR ($\lambda = 1030$ nm, IR) with pulse peak intensities ranging from 156 to 626 MW cm⁻². The SOSG probe is excited at 515 nm wavelength (Vis). The peak intensity of the 515-nm laser pulses is 1.22 MW cm⁻².

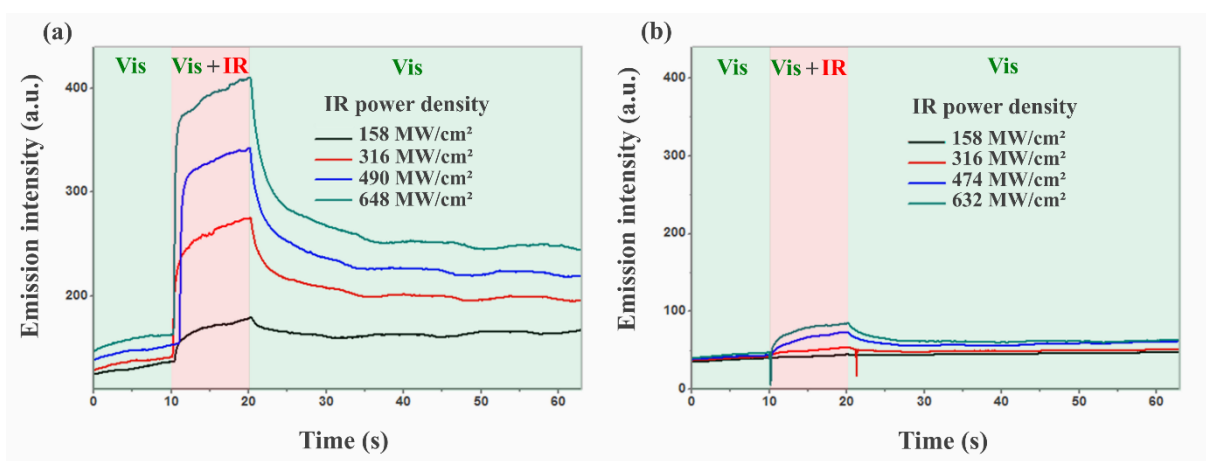


Fig. S6. DHR emission intensity in the presence of (a) PEGylated AuNRs and (b) AuNRs@SiO₂ acting as ROS photosensitizers, in water. The DHR reagent detects ¹O₂ and •OH. The DHR fluorescence is recorded before, during, and after the excitation of the NP longitudinal LSPR ($\lambda = 1030$ nm, IR) with pulse peak intensity ranging from 158 to 648 MW cm⁻². The DHR probe is excited at 515 nm wavelength (Vis). The peak intensity for the 515-nm laser pulses is 0.35 MW cm⁻².

IV. ROS production by bare AuNRs and AuNRs@SiO₂ with 5.0-nm and 8.7-nm silica shell

We analyzed further the results obtained with the two sets of silica shells, 8.7 and 5.0 nm average thickness (the AuNR core dimensions are then respectively 12.2 ± 1.3 nm diameter, 73.0 ± 8.3 nm length and 10.2 ± 1.0 nm diameter, $61.3 \text{ nm} \pm 7.2$ nm length). For this:

- The raw kinetics (Figs. 3 and 4 of the main article, S5 and S6 of the ESI) are corrected from the offset (baseline of the 515-nm illumination curves).
- The results are normalized to account for the varying optical density of the different AuNR and AuNR@SiO₂ solutions and the relative powers of the 515-nm illumination in the different experiments.
- The ROS production is evaluated as the ratio of the maximal value of the ROS generation rate reached for each incident IR power and the largest value obtained among all powers.

We then find the following trends:

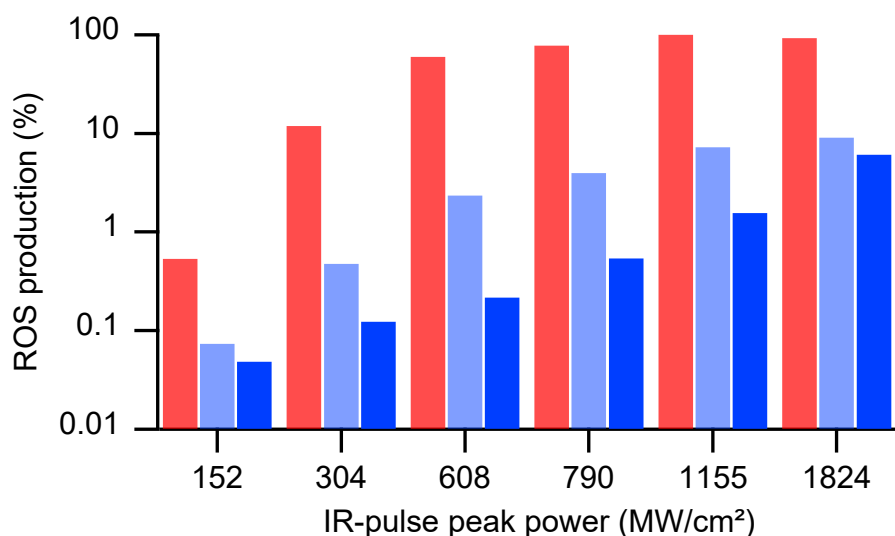


Fig. S7. ¹O₂ ROS production (probed by SOSG), relative to the maximum value, of PEGylated AuNRs (red), AuNRs@SiO₂ with 5.0-nm thick shell (light blue), and AuNRs@SiO₂ with 8.7-nm thick shell (marine blue) in water, for increasing IR-laser peak powers. The vertical axis is in log scale.

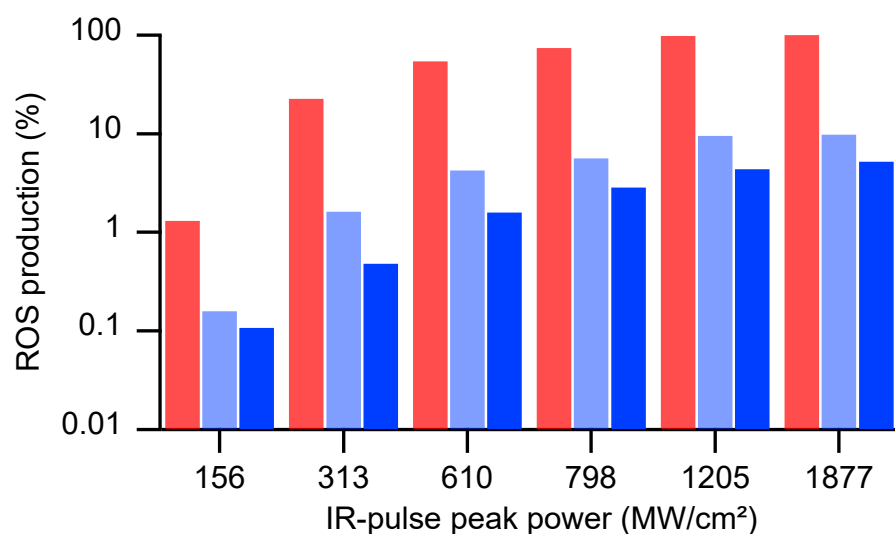


Fig. S8. ¹O₂ and •OH ROS production (probed by DHR), relative to the maximum value, of PEGylated AuNRs (red), AuNRs@SiO₂ with 5.0-nm thick shell (light blue), and AuNRs@SiO₂ with 8.7-nm thick shell (marine blue) in water, for increasing IR-laser peak powers. The vertical axis is in log scale.

Let us first notice that at high IR light intensity the production of ROS tends to saturate. The production of ROS is hindered by at least one order of magnitude when coating bare AuNRs with a 5.0- or 8.7-nm silica layer whatever the laser power within our range of investigation. Furthermore, the thicker the silica shell, the better the inhibition of ROS generation. The average inhibition efficiency (defined as the ratio of the ROS production attenuation after coating with silica and the initial ROS production of the bare AuNRs) is 92.7 ± 3.9 % for $^1\text{O}_2$ and 91.0 ± 1.9 % for $^1\text{O}_2$ and $\bullet\text{OH}$ in the case of a 5.0-nm silica shell, and 96.8 ± 3.7 % and 95.5 ± 2.1 % in the case of a 8.7-nm silica shell.

V. BEM numerical simulations - Extinction cross sections

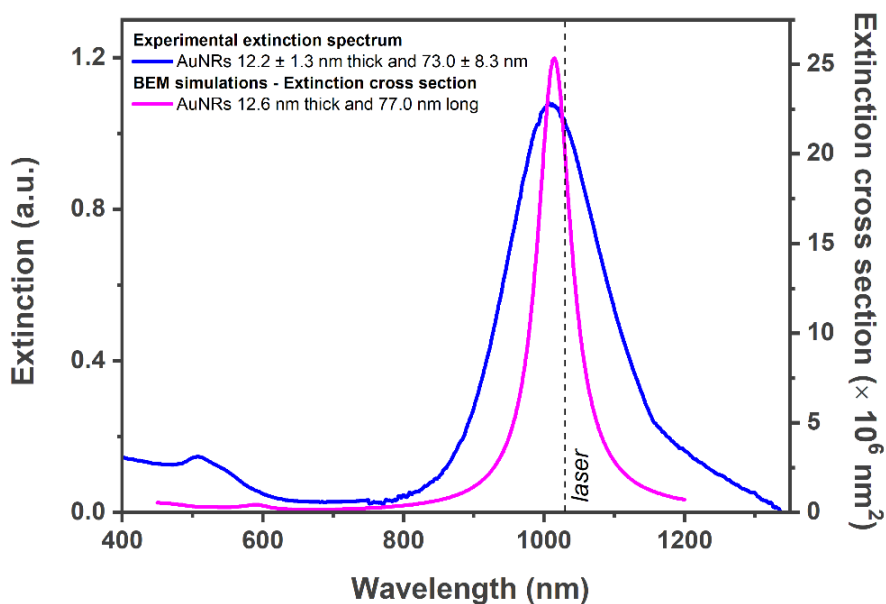


Fig. S9. Blue curve: Extinction spectrum of the PEGylated AuNRs used in the experiments presented in the article. The PEGylated AuNRs average dimensions are 12.2 ± 1.3 nm in diameter and 73.0 ± 8.3 nm in length. They display an effective longitudinal LSPR band peaking at 1013 nm. Purple curve: BEM simulation of the extinction cross section of an individual AuNR 12.6 nm thick and 77.0 nm long in water under longitudinal wave polarization. The longitudinal LSPR peak is obtained at 1014 nm. The vertical dashed line denotes the excitation laser wavelength.

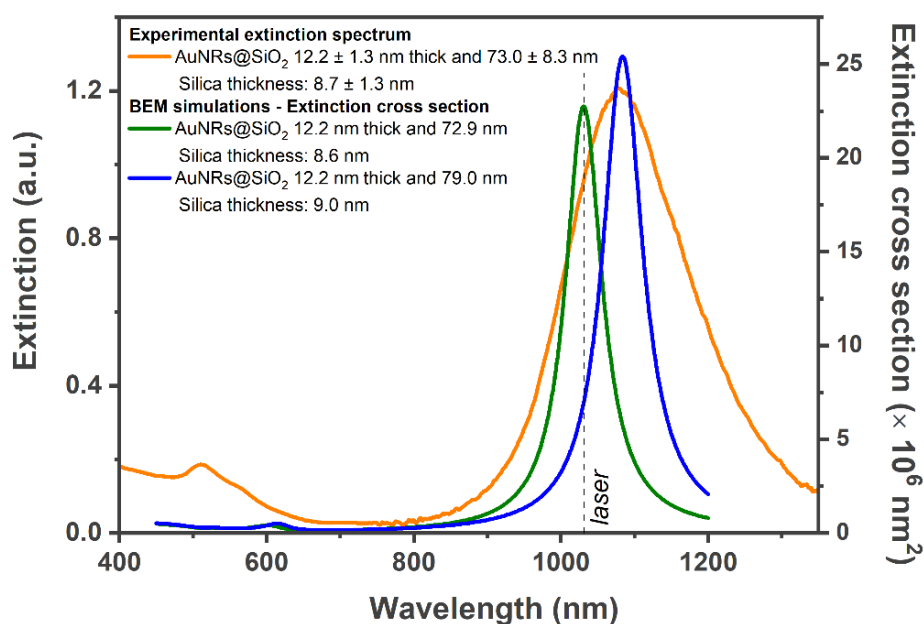


Fig. S10. Orange curve: Extinction spectrum of the AuNRs@SiO₂ solution used in the experiments presented in the article. The AuNRs@SiO₂ average dimensions are 12.2 ± 1.3 nm in diameter and 73.0 ± 8.3 nm in length, with a silica shell 8.7 ± 1.3 nm thick. The effective longitudinal LSPR of the AuNRs@SiO₂ set peaks at 1082 nm. Blue curve: BEM simulation of the extinction cross section spectrum of individual AuNRs@SiO₂ in water with LSPR at 1083 nm. Among the NP distribution in the experimental sample, some respond the most to the laser excitation at $\lambda=1030$ nm wavelength (vertical dashed line). BEM calculations show that AuNRs@SiO₂ 12.2 nm long and 72.9 nm wide, with a silica thickness of 8.6 nm, exhibit a longitudinal LSPR at this wavelength (green curve). These dimensions have then been used for the simulations.

VI. BEM numerical simulations – Maps of the optical near-field enhancement around the AuNR and AuNR@SiO₂

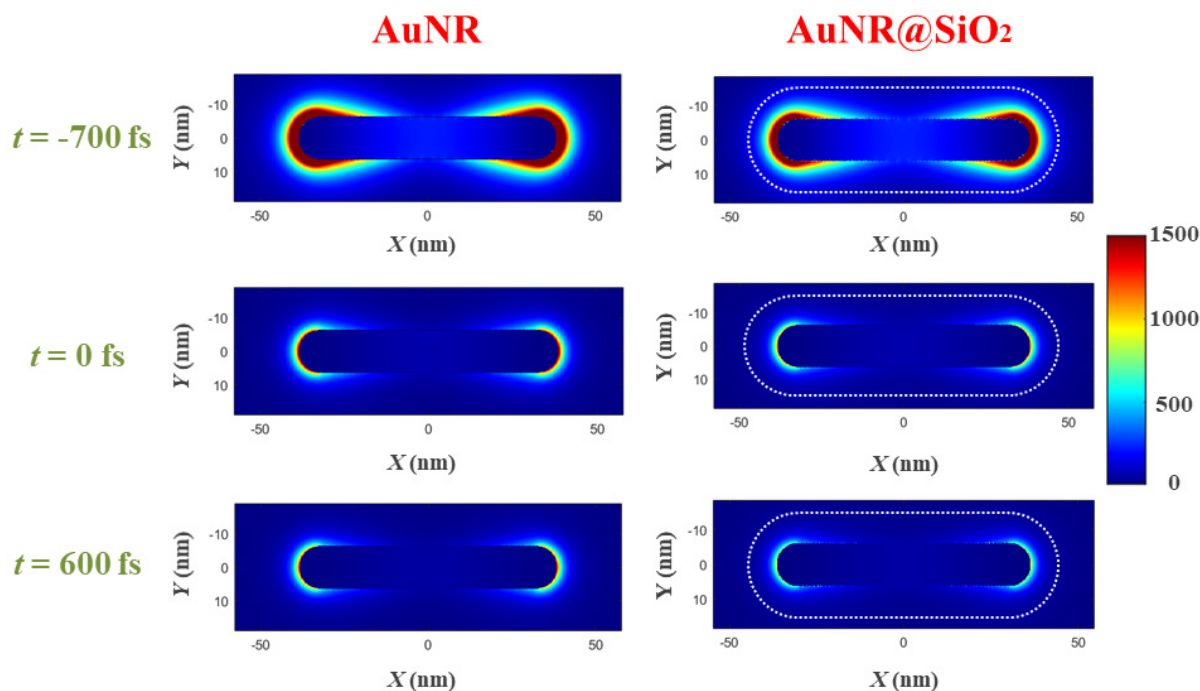


Fig. S11. Maps of the optical near-field enhancement $|E_p / E_0|^2$ (E_p and E_0 are respectively the local plasmonic field and the incident electric field) around a AuNR and a AuNR@SiO₂. The maps are collected before ($t = -700$ fs), at the maximum of ($t = 0$ fs) and after ($t = 600$ fs) the laser pulse. The simulations are carried out for an individual AuNR 12.6 nm thick and 77.0 nm long, and an individual AuNR@SiO₂ 12.2 nm thick and 72.9 nm long, with a silica thickness of 8.6 nm. The AuNR and AuNR@SiO₂ are excited at $\lambda=1030$ nm (IR), with a linear polarization parallel to the nanorod long axis.

Reference

1. T. Labouret, Irradiation laser ultrabrève de nanobâtonnets d'or individuels en milieu aqueux : photo-génération de phénomènes d'intérêt biomédical, PhD thesis, Université Paris-Saclay, 2016.